Analysis of Electromigration in Dual-Damascene Interconnect Structures

Roberto Lacerda de Orio, Hajdin Ceric, and Siegfried Selberherr

Institute for Microelectronics, TU Wien Gußhausstraße 27-29/E360, A-1040 Wien, Austria
e-mail: orio@iue.tuwien.ac.at

ABSTRACT

The effects of grain boundaries on electromigration failure are presented. The electromigration model incorporates the grain boundary as a separate medium which acts not only as fast diffusivity path for material transport but also absorbs and releases vacancies. Moreover, we analyze the void nucleation condition and its implication on electromigration failure is discussed. Our results show that high stress and a high vacancy concentration develop at the triple points formed on the interface between copper grains and the capping layer, where a void nucleation is likely to take place. This scenario of weak triple points in combination with a stress threshold also supports the mechanism of multiple void nucleation as it has been experimentally observed.

Index Terms: Electromigration, dual-damascene, interconnect.

1. INTRODUCTION

As the interconnect dimensions in modern integrated circuits continue to decrease, the metallization lines have become subject to very large current densities, accentuating the electromigration failure. Therefore, electromigration has become one of the most important reliability issues.

Blech [1, 2] was one of the first to explain the origin of the electromigration phenomena. In his experiments he discovered a critical product of interconnect line length and current density, below which no electromigration failure is observed. Kirchheim [3] proposed a physically based model in which the generation of stress in the grain boundaries during electromigration is caused by annihilation and generation of vacancies. Korhonen [4] proposed another physics-based analytical model for mechanical stress evolution during electromigration in a confined metal line described by a one-dimensional equation.

Since electromigration has been recognized as an important risk for interconnect reliability, engineers have been thinking about strategies for reducing or completely eliminating its effect. Independent of interconnect technology, there are basically two possibilities how to contest electromigration. The first one is choosing the appropriate materials or combination of these materials to produce preferable properties. Such efforts led from aluminum interconnects to aluminum-copper alloys, and later to pure copper interconnects. This material design for reliability also encompasses the choice of materials which surround the interconnect metal.

The copper interconnect in modern dual-damascene technology is completely embedded in a barrier and in a capping layer. Thus, the adhesion properties between these layers and copper are of crucial importance [5]. As experimental investigations have shown [6], the copper/capping layer interface acts as the dominant path for atomic diffusion in modern dual-damascene interconnects. However, several works have shown that grain boundary diffusion plays a significant role during electromigration and, therefore, cannot be neglected [7].

The interconnect microstructure depends on many parameters, such as the core material deposition technique, barrier material types and deposition techniques, copper seed layer deposition, line thickness and width. Also, the network of the grain boundaries influences material transport during electromigration in different ways:

• The diffusion of point defects inside the grain boundary is faster compared to the grain bulk diffusion, because a grain boundary generally exhibits a larger diversity of point defect migration mechanisms [8]. Moreover, the formation energies and migration

barriers for point defects in grain boundaries are lower than those for the lattice.

- Grain boundaries are locations of atomic flux divergence.
- Grain boundaries act as sites of annihilation and production of vacancies [9].

Therefore, the electromigration failure rate should depend on the grain size of the metallic film. While such a dependence is well known for aluminum interconnects, it is less pronounced for copper interconnects.

The main challenge in electromigration modeling and simulation is the diversity of the relevant physical phenomena. Electromigration induced material transport is also accompanied by material transport driven by the gradients of material concentration, mechanical stress, and temperature distribution. Furthermore, taking into account the effects of interfaces and grain boundaries as fast diffusivity paths imposes new challenges for electromigration modeling. A comprehensive, physics-based analysis of electromigration for modern copper interconnect lines can serve as the basis for deriving proper design rules, which will ensure higher steadfastness of interconnects against electromigration.

In this work we present the results of our investigations of the effect of grain boundaries on the electromigration failure mechanism. As basis for our analysis a comprehensive, multi-physics model of electromigration and accompanying effects is used. Our model reveals an improvement in two major points. First, there is a complete integration of the mechanical stress phenomena in connection with microstructural aspects in the classical multi-driving force model and, secondly, the developed finite element based scheme enables an efficient numerical solution of the three-dimensional formulation of the problem.

2. ELECTROMIGRATION MODELING

The transport of vacancies due to the gradient of vacancy concentration, electric field, gradient of temperature, and gradient of mechanical stress, respectively, is [10]

$$\vec{J}_v = -D_v\left(\nabla C_v + \frac{Z^* e}{k_B T} C_v \nabla \varnothing - \frac{Q^*}{k_B T^2} C_v \nabla T + \frac{f\Omega}{3k_B T} C_v \nabla tr(\vec{\sigma})\right), \qquad (1)$$

where D_v is the vacancy diffusion coefficient, C_v is the vacancy concentration, Z^*e is the effective charge, Q^* is the heat of transport, which determines the magnitude of matter fluxes in non-isothermal systems, f is the vacancy relaxation ratio, Ω is the atomic volume, tr $tr(\vec{\sigma})$ is the trace of the stress tensor, k_B is Boltzmann's constant, and T is the temperature.

In sites of flux divergence, vacancies will accumulate or vanish, and this vacancy dynamics is described by the continuity equation [10]

$$\frac{\partial C_v}{\partial t} = -\nabla.\vec{J_v} + G(C_v). \qquad (2)$$

The term $G(C_v)$ is a source function which models vacancy generation and annihilation processes and is considered only in interfaces and grain boundaries. This function has to comprise three processes:

- Exchange of point defects between adjacent grains.
- Exchange of point defects between grains and grain boundaries.
- Point defect formation/annihilation inside the grain boundaries.

A detailed analysis of this function in connection with the microstructure effect will be presented in Section 2.1.

Sarychev *et al.* [10] introduced the contribution of the local vacancy dynamics to stress build-up in a three-dimensional model of stress evolution during electromigration, which is given in terms of strain by [11]

$$\frac{\partial \varepsilon_{kk}}{\partial t} = \Omega\left[(1-f)\nabla . \vec{J_v} + fG(C_v)\right], \qquad (3)$$

where ε_{kk} is the trace of the strain vector.

2.1 Grain Boundaries

The grain boundary is treated as a separate medium capable of absorbing and releasing vacancies, where the vacancy dynamics is based on Fisher's model [12]. This model includes two mechanisms: vacancy diffusion in the grain boundary and material exchange between the grain boundary and the grain bulk. A schematic view of a grain boundary is depicted in Figure 1.

Fisher's expression for vacancy diffusion inside the grain boundary is

$$\frac{\partial C_v^{gb}}{\partial t} = -\frac{\partial J_v^{gb}}{\partial l} - \frac{1}{\delta}\left(J_v^2 - J_v^1\right), \qquad (4)$$

where C_v^{gb} is the grain boundary vacancy concentration, J_v^{gb} is the vacancy flux along a grain boundary distance l, δ is the grain boundary thickness, and J_v^1, J_v^2 are the fluxes from both sides of the grain boundary. From (4) one can see that the emission and absorption of vacancies are regulated by the fluxes J_v^1 and J_v^2, yielding the generation and recombination term

$$G = -\frac{1}{\delta}\left(J_v^2 - J_v^1\right). \qquad (5)$$

Following [13], we define the concentration of immobile vacancies which are trapped inside the grain

boundary as C_v^{im}. The flux from both sides of the grain boundaries can then be expressed as

$$J_v^1 = \omega_T \left(C_v^{eq} - C_v^{im}\right) . C_v^1 - \omega_R C_v^{im}, \quad (6)$$

$$J_v^2 = - \omega_T \left(C_v^{eq} - C_v^{im}\right) . C_v^2 - \omega_R C_v^{im}$$

where ω_T is the trapping rate of vacancies from both neighboring grains, ω_R is the release rate and C_v^1, C_v^2 are the vacancy concentrations on each side of the grain boundary.

C_v^{eq} is the equilibrium vacancy concentration inside the grain boundary, which is related to the stress by

$$C_v^{eq} = C_v^0 \, exp\left(\frac{\sigma_{nn}\Omega}{k_B T}\right), \quad (7)$$

where C_v^0 is the equilibrium vacancy concentration in the absence of stress and σ_{nn} is the stress component normal to the grain boundary. Using the immobile vacancy concentration definition, we can now reinterpret (5) as a function of the vacancies that are trapped in the grain boundary so that

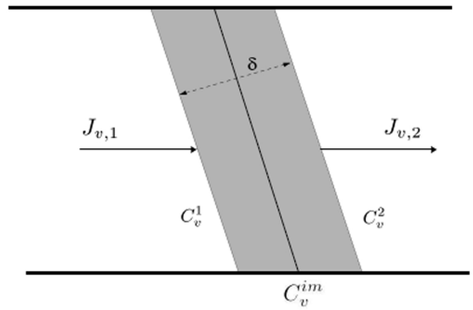

Figure 1. Grain boundary schematic

$$G = \frac{\partial C_v^{im}}{\partial t} = \frac{1}{\tau}\left[C_v^{eq} - C_v^{im}\left(1 + \frac{2\omega_R}{\omega_T\left(C_v^1 + C_v^2\right)}\right)\right], \quad (8)$$

with τ given by

$$\tau = \frac{\delta}{\omega_T\left(C_v^1 + C_v^2\right)} \quad . \quad (9)$$

Here, τ is the vacancy relaxation time and it characterizes the efficiency of the sites acting as vacancy sinks/sources. Smaller values of τ result in shorter times for the vacancy concentration to reach the steady state condition.

2.2. Void Nucleation Condition

From the early days of electromigration modeling, the void nucleation condition has been set based on the following two criteria:

- void nucleation after reaching a vacancy (atomic) concentration threshold [14];
- void nucleation after reaching a tensile stress threshold [15, 16].

However, a careful investigation based on classical nucleation theory has shown that these nucleation conditions, from a thermodynamic point of view, cannot be justified.

From the classical nucleation theory, in a strained single-phase material, a droplet of a second phase embryo is produced by spontaneous fluctuations, when the barrier energy ΔF^*, given by [17]

$$\Delta F^* = \frac{48\pi\gamma_m^3}{\left(tr(\vec{\sigma})\right)^2}, \quad (10)$$

for spherical embryos, is overcome. Here, γ_m is the surface free energy, and $tr(\vec{\sigma})$ is the trace of the applied stress field. If we assume a rather high hydrostatic pressure of 1 GPa [18] and take 1.72 J/m² as the surface free energy of copper [19], we obtain an energy barrier of 133 eV. Then, the number of critical embryos per unit volume can be calculated by [17]

$$Z^* = \frac{1}{\Omega n^*}\left(\frac{\Delta F^*}{3\pi k_B T}\right)^{1/2} exp\left(\frac{-\Delta F^*}{k_B T}\right), \quad (11)$$

where n^* is the number of vacancies in a critical embryo.

Critical embryos are spontaneously formed by the condensation of vacancies in stressed copper. However, the condensation process is reversible and, in most cases, the embryos completely dissolve in the surrounding lattice. The situation changes, when the critical embryo starts to accept additional free vacancies and the irreversible transition to an initial void is imminent [17]. Then, the nucleation rate is calculated as

$$I = \upsilon \, exp\left(-\frac{U_D}{k_B T}\right) Z^* \, n_S^*, \quad (12)$$

where υ is the frequency of vibration of the atoms, U_D is the activation energy of the jump process, and n_s^* is the number of vacancies in the matrix at the surface of the critical embryo.

For copper, the nucleation rate in the metal bulk is about 10^{-1396} $m^{-3}s^{-1}$. The nucleation rate dependence on temperature/stress is presented in Figure 2. Similar values can be obtained for nucleation at the interconnect sidewall, grain boundaries, and sidewall/grain boundary intersection. This means that a void nucleation by means of vacancy condensation for both, accelerated test conditions and realistic use conditions, is not possible.

An analysis carried out by Flinn [20] set a new framework for the understanding of void nucleation. The author considers a circular patch on the interface between copper and the capping layer with virtually no adhesion. Such an entity can actually be the pro-

duct of a surface defect or contamination [21]. As the stress in the line increases, the free metal surface is driven to accommodate a half-spherical void embryo. The stress threshold given by Clemens et al. [22] and Gleixner *et al.* [18] is

$$\sigma_{th} = \frac{2\gamma_m sin\ \theta_c}{R_p}, \tag{13}$$

where R_p is the radius of the adhesion-free patch and θ_c is the equilibrium contact angle between the void and the sidewall.

For stresses $\sigma < \sigma_{th}$ an energy barrier exists between the embryo and a stable-growing void. If the stress is larger than the threshold value ($\sigma > \sigma_{th}$), the free energy monotonically decreases with the void volume and the energy barrier vanishes. If we now assume the adhesion free patch with a radius of 10 nm, approximately 20 atoms, and $\theta c = \pi/2$, we obtain $\sigma_{th} \sim 344$ MPa. Such a stress level can already be reached by thermal stress [23] in modern interconnects.

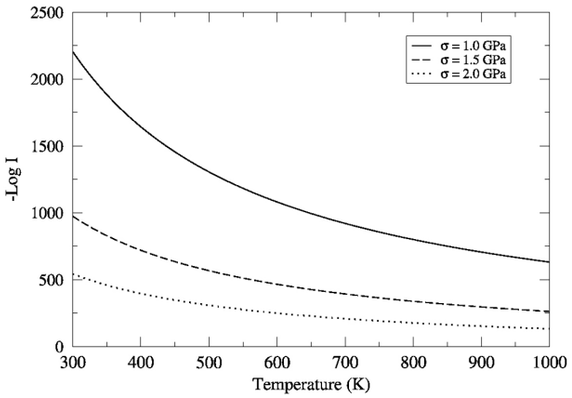

Figure 2. Nucleation rate dependence on hydrostatic stress and temperature. Even a very high temperature can not significantly increase the nucleation rate. The parameters were obtained from [18].

3. SIMULATION PROCEDURE

The model presented in the previous section is numerically solved by the finite element method implemented in an in-house code for three-dimensional structures. The solving algorithm is depicted in Figure 3. Each model is handled according to a unique priority list, so that the calculated attributes are transferred from the model of higher priority to the model of lower priority.

The simulation starts with the solution of the electro-thermal problem, which is the coupled system of the Laplace and the Fourier equation

$$\nabla \cdot (\gamma_E \nabla V) = 0\,, \tag{14}$$

$$\nabla \cdot (\gamma_T \nabla T) = c_p \rho_m \frac{\partial T}{\partial t} - \gamma_E |\nabla V|^2,$$

where γ_E is the electrical conductivity, γ_T is the thermal conductivity, c_p is the specific heat, and ρ_m is the density. Then, the vacancy dynamics in the presence of grain boundaries is determined by solving the continuity equation

$$\frac{\partial C_v}{\partial t} = -\nabla \cdot \vec{J_v} + \frac{1}{\tau}\left[C_v^{eq} - C_v^{im}\left(1 + \frac{2\omega_R}{\omega_T\left(C_v^1 + C_v^2\right)}\right)\right]. \tag{15}$$

Finally, the corresponding strain and stress are determined via the solution of (3) in combination with Hooke's law and the mechanical equilibrium equation, respectively

$$\sigma_{ij} = \sum_{ijkl} C_{ijkl}\, \varepsilon_{kl}, \tag{16}$$

$$\nabla \cdot \vec{\sigma} = 0$$

where C_{ijkl} is the elastic modulus tensor.

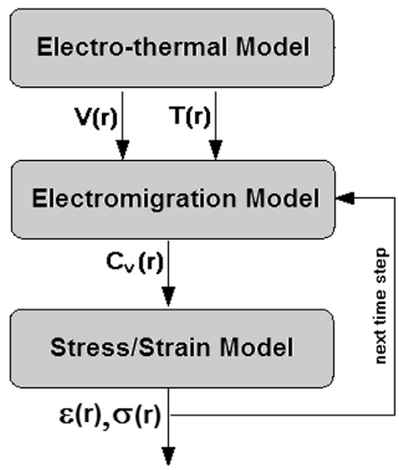

Figure 3. The complete solving procedure. The electromigration and the mechanical problem are solved each time step.

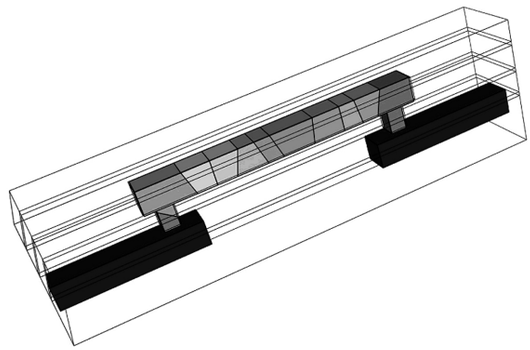

Figure 4. Three-dimensional interconnect structure with polycrystalline copper metallization.

$D_{bulk} = 0.52\ exp\ (-1.1eV / k_BT)\ cm^2/s$

4. RESULTS AND DISCUSSION

We have applied the model presented in this work to an interconnect layout which has been extensively used for accelerated electromigration tests [6]. This layout, as shown in Figure 4, is typical for dual-damascene 0.18 μm technologies. The copper microstructure has been set according to results of EBSD (Electron Backscatter Diffraction) measurements [24].

The peak values of stress are extracted from three extraction cylinders (C1, C2, and C3), which are presented in Figure 5a. The solution of the electro-thermal problem sets the operating conditions for electromigration simulation. The applied mechanical, thermal, and electrical boundary conditions are presented in Figure 5b. The temperature is set constant at T_0 = 673 K and the voltage is V_0 =10 mV. This results in a current density of 10 MA/cm^2.

In dual-damascene technologies the interface copper/capping (etch-stop) layer is recognized as the fastest material transport path when standard capping dielectrics SiNx are used [6]. In order to properly include the effect of fast diffusivity paths, grain boundary, barrier, and capping layer diffusivities are set to $10^2 D_{bulk}$, $10^2 D_{bulk}$, and $10^5 D_{bulk}$, respectively. The applied bulk diffusivity is $D_{bulk} = 0.52\ exp\ (-1.1eV / k_BT)\ cm^2/s$ (25).

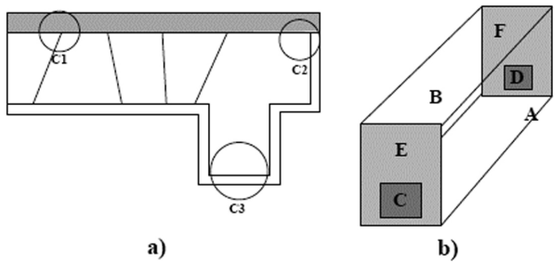

Figure 5. a) Peak values of hydrostatic stress and vacancy concentration values are extracted from cylinders C1, C2, and C3. b) Applied boundary conditions: A, B: fixed temperature T_0=673 K; C, D: voltage V_0=10 mV; upstream electromigration, i.e. electrons flow from C3 to C1; E, F: mechanically fixed.

As previously discussed, in order that a void nucleation can occur, the development of high tensile stress in a site of a local interface defect is necessary. Therefore, we monitor the hydrostatic stress development at the points C1, C2, and C3. A representative excerpt of the stress dynamics is shown in Figure 6. The distribution of the vacancy concentration and tensile stress are presented in Figure 7 and Figure 8, respectively.

We have observed that until approximately 10 min, the peak tensile stress and the vacancy concentration exhibit nearly exponential growth. After this phase the peak vacancy concentration increases only slightly and the peak tensile stress grows linearly. Such

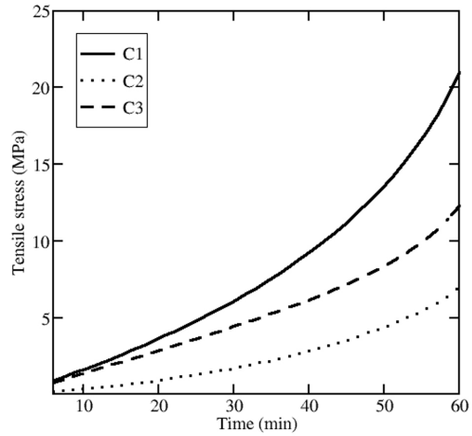

Figure 6. Time evolution of tensile hydrostatic stress at three spots of the interconnect.

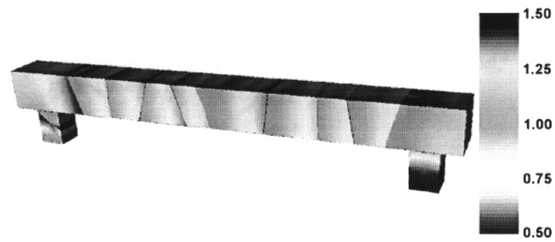

Figure 7. Vacancy distribution (in 10^{16} cm^{-3}). Right is the cathode end of the interconnect.

a behavior was already observed by Kirchheim [3], where it is called quasi steady state. After this quasi steady state a rapid growth of stress and vacancy concentration takes place.

As observed by Vairagar *et al.* [6], under operating conditions similar to our simulations, the first void nucleation occurs in less than 2 hours. According to our results, at this time we have already rapid stress growth and a stress level of 70 MPa at the triple point C1.

We can see that high values of the tensile stress tensor component σ_{yy}, which is orthogonal to the capping layer interface, can be observed at the capping layer interface in the vicinity of triple point intersections with grain boundaries. The coincidence of high vacancy concentration and high tensile stress values at such triple points indicates that these regions are prone to void nucleation, as they are natural places of weak adhesion. This assumption was also expressed in the discussion of results of accelerated tests in [6], [24]. Moreover, these works show that voids initially nucleate at the interface between the copper and the capping layer far away from the cathode. Then, these voids migrate in the direction opposite to the electron flow, toward the cathode end of the line, where they agglomerate and coalesce to form a void which spans the line, causing the failure. Our results indicate that the scenario of weak triple points in combination with a stress threshold supports such a mechanism of mul-

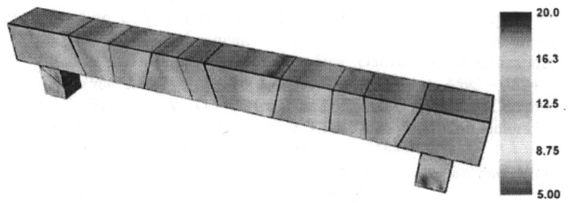

Figure 8. Tensile stress distribution (in MPa).

tiple void nucleation. As Figure 8 shows, peak tensile stress develops simultaneously at different intersections of grain boundaries and the capping layer.

5. CONCLUSION

We presented an electromigration model which takes into account all relevant driving forces for material transport with a special focus on the effects of the grain boundaries, which act not only as fast diffusivity paths but also as sites for vacancy generation and recombination. A detailed analysis of void nucleation conditions is given and the consequences for electromigration simulation are discussed. The model was implemented into a three-dimensional simulation tool based on an efficient finite element code.

The simulated dynamics of the proposed electromigration model is in good agreement with the experimental observations, reproducing typical characteristics of the electromigration failure. The role of microstructure is readily recognized, since we can observe peaks of stress and vacancy concentration located at triple points formed by the intersection of grain boundaries with the capping layer. Based on the void nucleation analysis we presented, the high stress developed at such sites makes them prone to void nucleation. Furthermore, the mechanism of multiple void nucleation can be also described by the model.

ACKNOWLEDGEMENTS

Support by the Austrian Science Fund with the project P18825-N14 is gratefully acknowledged.

REFERENCES

[1] I. A. Blech and C. Herring, "Stress Generation by Electromigration," J. Appl. Phys., vol. 29, no. 3, August 1976, pp. 131 – 133.
[2] I. A. Blech and K. L. Tai, "Measurement of Stress Gradients Generated by Electromigration," Appl. Phys. Lett., vol. 30, no. 8, April 1977, pp. 387 – 389.
[3] R. Kirchheim, "Stress and Electromigration in Al-Lines of Integrated Circuits," Acta Metall. Mater., vol. 40, no. 2, 1992, pp. 309 – 323.
[4] M. A. Korhonen, P. Borgesen, K. N. Tu, and C. Y. Li, "Stress Evolution due to Electromigration in Confined Metal Lines," J. Appl. Phys., vol. 73, no. 8, April 1993, pp. 3790 – 3799.
[5] E. Zschech, M. A. Meyer, S. G. Mhaisalkar, A. V. Vairagar, A. Krishnamoorthy, H. J. Engelmann, and V. Sukharev, "Effect of Interface Modification on EM-Induced Degradation Mechanisms in Copper Interconnects," Thin Solid Films, vol. 504, 2006, pp. 279 – 283.
[6] A. V. Vairagar, S. G. Mhaisalkar, A. Krishnamoorthy, K. N. Tu, A. M. Gusak, M. A. Mayer, and E. Zschech, "In Situ Observation of Electromigration-Induced Void Migration in Dual-Damascene Cu Interconnect Structures," Appl. Phys. Lett., vol. 85, no.13, September 2004, pp. 2502 – 2504.
[7] L. Arnaud, T. Berger, and G. Reimbold, "Evidence of Grain-Boundary versus Interface Diffusion in Electromigration Experiments in Copper Dual Damascene Interconnects," J. Appl. Phys., vol. 93, no. 1, January 2003, pp. 192 – 204.
[8] M. R. Sorensen, Y. Mishin, and A. F. Voter, "Diffusion Mechanisms in Cu Grain Boundaries," Phys. Rev. B, vol. 62, no. 6, August 2000, pp. 3658 – 3673.
[9] R. W. Balluffi, "Grain Boundary Diffusion Mechanisms in Metals," Metall. Trans. A, vol. 13A, December 1982, pp. 2069 – 2095.
[10] M. E. Sarychev, Y. V. Zhitnikov, L. Borucki, C. L. Liu, and T. M. Makhviladze, "General Model for Mechanical Stress Evolution During Electromigration," J. Appl. Phys., vol. 86, no. 6, September 1999, pp. 3068 – 3075.
[11] H. Ceric, R. Heinzl, C. Hollauer, T. Grasser, and S. Selberherr, "Microstructure and Stress Aspects of Electromigration Modeling," in Stress-Induced Phenomena in Metallization, 2006, American Institute of Physics, pp. 262 – 268.
[12] J. C. Fisher, "Calculation of Diffusion Penetration Curves for Surface and Grain Boundary Diffusion," J. Appl. Phys., vol. 22, no. 1, January 1951, pp. 74 – 77.
[13] F. Lau, L. M. Mader, C. Mazure, Ch. Werner, and M. Orlowski, "A Model for Phosphorous Segregation at the Silicon-Silicon Dioxide Interface," Appl. Phys. A, vol. 49, 1989, pp. 671 – 675.
[14] O. Kraft and E. Arzt, "Current Density and Line Width Effects in Electromigration: a New Damage-Based Lifetime Model," Acta Mater., vol. 46, no. 11, 1998, pp. 3733 – 3743.
[15] C. L. Gan, C. V. Thompson, K. L. Pey, W. K. Choi, H. L. Tay, B. Yu, and M. K. Radhakrishnan, "Effect of Current Direction on the Lifetime of Different Levels of Cu Dual-Damascene Metallization," Appl. Phys. Lett., vol. 79, no. 27, December 2001, pp. 4592 – 4594.
[16] J. T. Trattles, A. G. O'Neill, and B. C. Mecrow, "Computer Simulation of Electromigration in Thin-Film Metal Conductors," J. Appl. Phys., vol. 75, no. 12, June 1994, pp. 7799 - 7804.
[17] J. W. Christian, The Theory of Transformations in Metal and Alloys, Pergamon, 2002, p. 436.
[18] R. J. Gleixner, B. M. Clemens, and W. D. Nix, "Void Nucleation in Passivated Interconnect Lines: Effects of Site Geometries, Interfaces, and Interface Flaws," J. Mater. Res., vol. 12, August 1997, pp. 2081 – 2090.
[19] D. A. Porter and K. E. Easterling, Phase Transformations in Metals and Alloys, 2nd ed., Stanley Thornes Publishers Ltd, 2000, p. 113.
[20] P. A. Flinn, "Mechanical Stress in VLSI Interconnections: Origins, Effects, Measurement, and Modeling," MRS Bulletin, vol. 20, November 1995, pp. 70 – 73.
[21] E. Zschech, H. J. Engelmann, M. Meyer, V. Kahlert, A. V. Vairagar, S. G. Mhaisalkar, A. Krishnamoorthy, M. Yan, K. N. Tu, and V. Sukharev, "Effect of Interface Strength on Electromigration Induced Inlaid Copper Interconnect Degradation: Experiment and Simulation," Zeitschrift für Metallkunde, vol. 96, no. 9, 2005, pp. 966 – 971.
[22] B. M. Clemens, W. D. Nix, and R. J. Gleixner, "Void Nucleation on a Contaminated Patch," J. Mater. Res., vol. 12, August 1997, pp. 2038 – 2042.
[23] Z. Jing, M. O. Bloomfield, L. Jian-Qiang, R. J. Gutmann, and T. S. Cale, "Modeling Thermal Stresses in 3-D IC Interwafer Interconnects," IEEE Trans. Sem. Man., vol. 19, no. 4, November 2006, pp. 437 – 448.
[24] E. Zschech and V. Sukharev, "Microstructure Effect on EM-Induced Copper Interconnect Degradation: Experiment and Simulation," Microelectron. Eng., vol. 82, 2005, pp. 629 – 638.
[25] V. Sukharev, E. Zschech, and W. D. Nix, "A Model for Electromigration-I nduced Degradation Mechanisms in DualInlaid Copper Interconnects: Effect of Microstructure," J. Appl. Phys., vol. 102, 2007, pp. 053505-1 – 053505-7.